RESEARCH REPORTS
Biological

K. Iida[1], T. Takeda-Kawaguchi[1], M. Hada[2], M. Yuriguchi[2], H. Aoki[2], N. Tamaoki[1], D. Hatakeyama[1], T. Kunisada[2], T. Shibata[1], and K. Tezuka[2]*

[1]Department of Oral and Maxillofacial Science, Gifu University Graduate School of Medicine, 1-1 Yanagido, Gifu City, Gifu 501-1194, Japan; and [2]Department of Tissue and Organ Development, Gifu University Graduate School of Medicine, 1-1 Yanagido, Gifu City, Gifu 501-1194, Japan; *corresponding author, tezuka@gifu-u.ac.jp

J Dent Res 92(10):905-910, 2013

Hypoxia-enhanced Derivation of iPSCs from Human Dental Pulp Cells

ABSTRACT

Hypoxia enhances the reprogramming efficiency of human dermal fibroblasts to become induced pluripotent stem cells (iPSCs). Because we showed previously that hypoxia facilitates the isolation and maintenance of human dental pulp cells (DPCs), we examined here whether it promotes the reprogramming of DPCs to become iPSCs. Unlike dermal fibroblasts, early and transient hypoxia (3% O_2) induced the transition of DPCs to iPSCs by 3.3- to 5.1-fold compared with normoxia (21% O_2). The resulting iPSCs closely resembled embryonic stem cells as well as iPSCs generated in normoxia, as judged by morphology and expression of stem cell markers. However, sustained hypoxia strongly inhibited the appearance of iPSC colonies and altered their morphology, and antioxidants failed to suppress this effect. Transient hypoxia increased the expression levels of *NANOG* and *CDH1* and modulated the expression of numerous genes, including those encoding chemokines and their receptors. Therefore, we conclude that hypoxia, when optimized for cell type, is a simple and useful tool to enhance the reprogramming of somatic cells to become iPSCs.

KEY WORDS: cell hypoxia, stem cells, odontoblasts, cadherins, microarray analysis, chemokines.

DOI: 10.1177/0022034513502204

Received April 9, 2013; Last revision July 19, 2013; Accepted July 30, 2013

A supplemental appendix to this article is published electronically only at http://jdr.sagepub.com/supplemental.

INTRODUCTION

Human dental pulp cells (DPCs) are present in dental pulp tissues, and function as stem/progenitor cells through their ability to self-renew and differentiate into restricted-lineages (Gronthos *et al.*, 2000, 2002; Takeda *et al.*, 2008). We previously reported that retroviral transduction of 4 transcription factors (*OCT3/4, SOX2, KLF4*, and *c-MYC*) can reprogram DPCs into induced pluripotent stem cells (iPSCs) that closely resemble embryonic stem cells (ESCs). These findings suggested that an iPSC bank can be established from DPCs as a valuable resource for regenerative medicine (Tamaoki *et al.*, 2010; Okita *et al.*, 2011). However, dental pulp tissues isolated from aged donors (45-68 yrs) are smaller, form fewer DPC colonies in culture, and have diminished proliferative capacity (Iida *et al.*, 2010). Therefore, to establish iPSCs from a wide range of donors, such as patients with chronic diseases specific to later stages of life, it is important to improve reprogramming and colony-forming efficiencies of primary cultures.

Human peripheral tissues reside in a low-oxygen-tension environment. Therefore, low-oxygen tension is suitable for establishing and maintaining human somatic cells (Packer and Fuehr, 1977; D'Ippolito *et al.*, 2006). Rat incisor pulp tissue is surrounded by hard dentin tissue, and its oxygen tension (23.2 mm Hg, 3% O_2) is lower than that of air (Yu *et al.*, 2002). We previously showed that hypoxia (3% O_2) enhances proliferation and inhibits differentiation of human DPCs (Iida *et al.*, 2010). Recently, exposure to hypoxia was reported to enhance the reprogramming of human dermal fibroblast cells (DFs) (Yoshida *et al.*, 2009). Therefore, we reasoned that hypoxia might enhance the reprogramming of DPCs toward iPSCs. Thus, the goal of the present study was to test the effect of hypoxia on reprogramming human DPCs.

MATERIALS & METHODS

Cell Culture and Generation of iPSCs

Human DPCs, collected from patients at Gifu University Hospital who provided informed consent, were isolated and cultured by previously reported techniques (Gronthos *et al.*, 2000) and modifications as described in the Appendix. Following the guidelines for the generation of human iPSCs approved by the Institutional Review Board of Gifu University, we used DPCs from three donors (DP31, 14-year-old girl; DP54, 19-year-old man; and

Table 1. Genes Up-regulated (Hypoxia>Normoxia) or Down-regulated (Hypoxia<Normoxia) by >5-fold

Hypoxia>Normoxia			Hypoxia<Normoxia		
Gene Symbol	GenBank Accession Number	Fold-increase	Gene Symbol	GenBank Accession Number	Fold-increase
ANKRD24	NM_133475	38.43	*CXCR3*	NM_001504	10.91
CBLC	NM_012116	30.23	*MKRN3*	NM_005664	10.65
GFRA2	NM_001495	25.99	*GTSF1*	NM_144594	7.29
ATP9A	NM_006045	17.16	*CXCL1*	NM_001511	7.22
EGLN3	NM_022073	12.33	*CPA2a*	NM_001869	7.14
SORBS1	AK022468	8.91	*RGS18*	NM_130782	6.28
ANGPTL4	NM_139314	8.88	*OLAH*	NM_001039702	6.20
LILRA3	NM_006865	8.81	*FTMT*	NM_177478	6.14
PTPRB	NM_002837	7.96	*IL8*	NM_000584	5.74
SFTPA1	NM_005411	7.95	*KRTAP3-2*	NM_031959	5.11
CCR4	NM_005508	7.38			
OCLN	NM_002538	7.12			
SMPD3	NM_018667	7.02			
CA9	NM_001216	6.45			
IGFBP3	NM_001013398	6.37			
INHBB	NM_002193	6.34			
CDH1	NM_004360	5.75			
AQP1	NM_198098	5.56			
FAM189A2	NM_004816	5.45			
MCHR1	NM_005297	5.30			
APLN	NM_017413	5.18			

DP185, 62-year-old man) for generating iPSCs within 10 passages. Using a retroviral vector, we generated iPSCs that express the transcription factors encoded by *OCT3/4, SOX2, KLF4*, and *c-MYC* according to a published protocol (Takahashi *et al.*, 2007; Tamaoki *et al.*, 2010). To determine the reprogramming efficiency of DPCs under hypoxia, we cultured these cells in atmospheres containing either 21% O_2 or 3% O_2 and analyzed them according to the time schedule described in the Appendix. At 6 days post-infection, the cells were seeded onto feeder layers (see Appendix) and cultured in 21% O_2. On day 21, we counted the number of human ESC-like colonies and alkaline phosphatase (ALP)-positive colonies and isolated total RNA from the cells to determine the level of *NANOG* expression. To characterize iPSCs, we selected ESC-like colonies from days 14 to 21 and cultured them in 21% O_2. Assays were performed in triplicate, and the values of average and standard deviation (SD) were calculated. Student's *t* test was used for determining significance. A human ESC line (KhES01) was obtained from Kyoto University (Kyoto, Japan) and cultured on mitomycin C-treated SNL feeder layers (SNL cell line obtained from Sanger Institute, Cambridge, UK) in Primate ES cell medium (ReproCell, Tokyo, Japan) supplemented with 4 ng/mL basic fibroblast growth factor (Wako, Osaka, Japan).

Quantitative Real-time Polymerase Chain-reaction (RT-PCR)

RNA extraction (RNeasy Plus Mini Kit; Qiagen, Valencia, CA, USA) and RT-PCR (Thermal Cycler Dice Real Time System TP800; Takara, Shiga, Japan) were performed as described previously (Takeda *et al.*, 2008). The mRNA data were normalized to those of *GAPDH* and used to calculate expression coefficients. Primer sequences are shown in Appendix Table 1. Primers used for *OCT3/4, SOX2*, and *KLF4* specifically detect the endogenous transcripts (Takahashi *et al.*, 2007). For comparison of the expression levels of *CDH1* (E-cadherin) and *CXCR3* in DPCs exposed to normoxia and hypoxia, DPCs from the three donors were transduced as described above or not and then cultured for 6 days under 21% O_2 or 3% O_2. Expression levels of *CDH1* and *CXCR3* mRNA were assessed by RT-PCR at day 6 post-infection.

Immunohistochemistry

The cells were fixed with 4% paraformaldehyde for 15 min and treated with phosphate-buffered saline (PBS) containing 2% normal goat or donkey serum (Wako), 0.5% BSA (Sigma-Aldrich, St. Louis, MO, USA), and 0.2% Triton X-100 (Wako) for 30 min. The primary and secondary antibodies are shown in the Appendix. Nuclei were stained with 4′,6-diamidino-2-phenylindole (DAPI) (Merck Millipore, Billerica, MA, USA).

Teratoma Formation Assays

Teratoma formation assays were performed as reported (Takahashi *et al.*, 2007; Watanabe *et al.*, 2007). Briefly, 3×10^5 iPSCs were injected by means of a Hamilton syringe into the testes of six-week-old immunodeficient nude mice (BALB/c nu/nu; CLEA, Tokyo, Japan). Twelve wks after injection, tumors were dissected and fixed with PBS containing 4% paraformal-

dehyde. Paraffin-embedded tissues were sectioned (3 μm) with a microtome (TU-213, YAMATO KOUKI, Asaka, Japan) and stained with hematoxylin and eosin.

Microarray Analysis

DPCs from three donors (DP31, DP54, and DP185) that had been induced with the reprogramming factors were cultured in atmospheres of 21% O_2 or 3% O_2, according to the time schedule for hypoxic assessment described above. Total RNA was isolated with an RNeasy Plus Mini Kit (Qiagen) on day 6 after transduction. The cDNA microarray analysis was performed as described in the Appendix. The level of gene expression was determined by use of Gene Spring GX11.5 (Agilent Technologies, Santa Clara, CA, USA). The raw microarray data are deposited in the National Center for Biotechnology Information Gene Expression Omnibus (GEO Series GSE45872; http://www.ncbi.nlm.nih.gov/geo/).

Statistical Analysis

Data are presented as the mean ± SD. The differences in mean values were evaluated by the *t* test after evaluation of variances (Microsoft Excel). For RT-PCR, the mean and standard deviation of the expression coefficient were calculated with Thermal Cycler Dice® Real Time System Software Ver. 4.02 (Takara).

RESULTS

Hypoxia Enhances Reprogramming of DPCs

With a retrovirus vector, *OCT3/4, SOX2, KLF4*, and *c-MYC* were introduced into DPCs isolated from three individuals (DP31, DP54, and DP185), and 24 hrs later the cells were cultured under hypoxia (3% O_2) for 6 days and re-plated onto SNL feeder cells in an atmosphere containing 21% O_2 for an additional 14 days. Prolonged exposure to hypoxia after passage suppressed colony formation and altered the appearance of the ESC-like colonies. These colonies either became less compact (Appendix Fig. 1A) or their morphology was altered by the presence of peripheral spindle-like cells (Appendix Fig. 1B). However, exposure of DPCs to hypoxia for only the first 6 days significantly increased the number of ALP-positive (1.9- to 3.2-fold) and ESC-like colonies (3.3- to 5.1-fold, Fig. 1A). The expression levels of *NANOG* significantly increased, suggesting that this transient hypoxia enhanced reprogramming of the cells (Fig. 1B). There was a marked increase in the ratio of ESC-like colonies to ALP-positive cells generated from DPCs from a 62-year-old donor. This time schedule differed from that used in a previous study demonstrating that exposure of human DFs to 5% O_2 for 7 to 21 days of reprogramming enhanced generation of iPSCs (Yoshida *et al.*, 2009).

To investigate why prolonged cultivation of DPCs under 3% O_2 strongly suppressed colony formation and expansion, we checked the effect of hypoxia on established DPC-derived iPSCs. The growth of iPSCs established from DPCs did not change significantly in 3% O_2, suggesting that the morphology and proliferation of iPSCs were not affected once reprogramming was completed (Appendix Fig. 1C). We next cultured DPCs

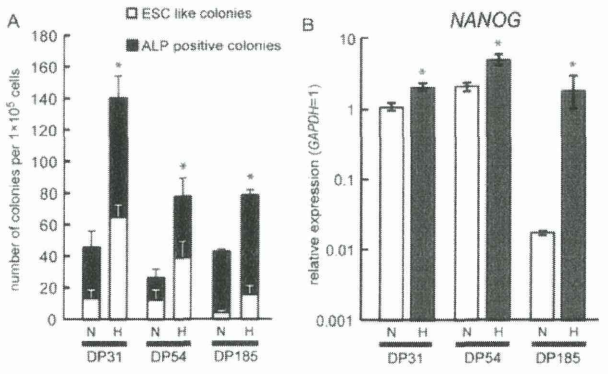

Figure 1. Generation of iPSCs under hypoxia. **(A)** Numbers of ESC-like colonies (white) and ALP-positive colonies (black) generated from 1 × 10^5 DPCs on day 21 after retroviral transduction. We transduced DPCs from three donors (DP31, DP54, and DP185) with retroviral expression vectors containing the genes encoding 4 programming factors (*OCT3/4, SOX2, KLF4*, and *c-MYC*), and incubated them in atmospheres of either 21% O_2 (N) or 3% O_2 (H) 1 to 6 days after virus infection, re-seeded them onto SNL feeder cells on day 6, and then incubated them in an atmosphere of 21% O_2. Mean numbers of colonies from 3 experiments (n = 3) are shown with error bars indicating SD; $*p < .05$ compared with 21% O_2. **(B)** The levels of *NANOG* expression were quantified by RT-PCR. Error bars indicate the SD obtained from triplicate measurements.

exposed to hypoxia for 2 days and observed increased levels of reactive oxygen species (ROS) (Appendix Fig. 2A). When DPCs were subjected to hypoxia, ROS generation was suppressed by anti-oxidants such as vitamins C and E (data not shown); however, when we generated iPSCs under 3% O_2 in the presence of these anti-oxidants for 21 days, we did not detect an increase in the induction of iPSCs (Appendix Fig. 2B), suggesting that ROS generation did not account for the adverse effects of sustained hypoxia. We conclude, therefore, that transient exposure to hypoxia at an early stage of reprogramming had a positive effect on DPCs, which was different from the effect on DFs.

The iPSC colonies were characterized by their ESC-like morphology and ALP activity (Figs. 2A, 2B, and Appendix Table 2). They were positive for OCT3/4, SSEA-4, TRA1-60, and TRA1-81, and negative for SSEA-1 (Figs. 2C-2G and Appendix Table 2). RT-PCR analysis showed that expression of *NANOG* and *REX1* was comparable with that of human ESCs, and endogenous *OCT3/4, SOX2*, and *KLF4* were also expressed (Fig. 2H). These cells also formed teratomas in nude mice, suggesting that they possess the characteristics of iPSCs (Figs. 2I-2K).

Effect of Transient Hypoxia Treatment on Gene Expression in DPCs

To assess the responses of DPCs to hypoxia, we first determined the levels of HIF-1α expression by cultures of DPCs exposed to hypoxia for 2, 4, and 24 hrs. The expression of HIF-1α increased transiently, suggesting a relatively rapid adaptation of the cells to hypoxia within 48 hrs (data not shown). To investigate the effect of oxygen concentration on global gene expression, we compared DPCs cultured for 6 days under hypoxia and normoxia (Appendix Figs. 3 and 4). Under hypoxia, the expression

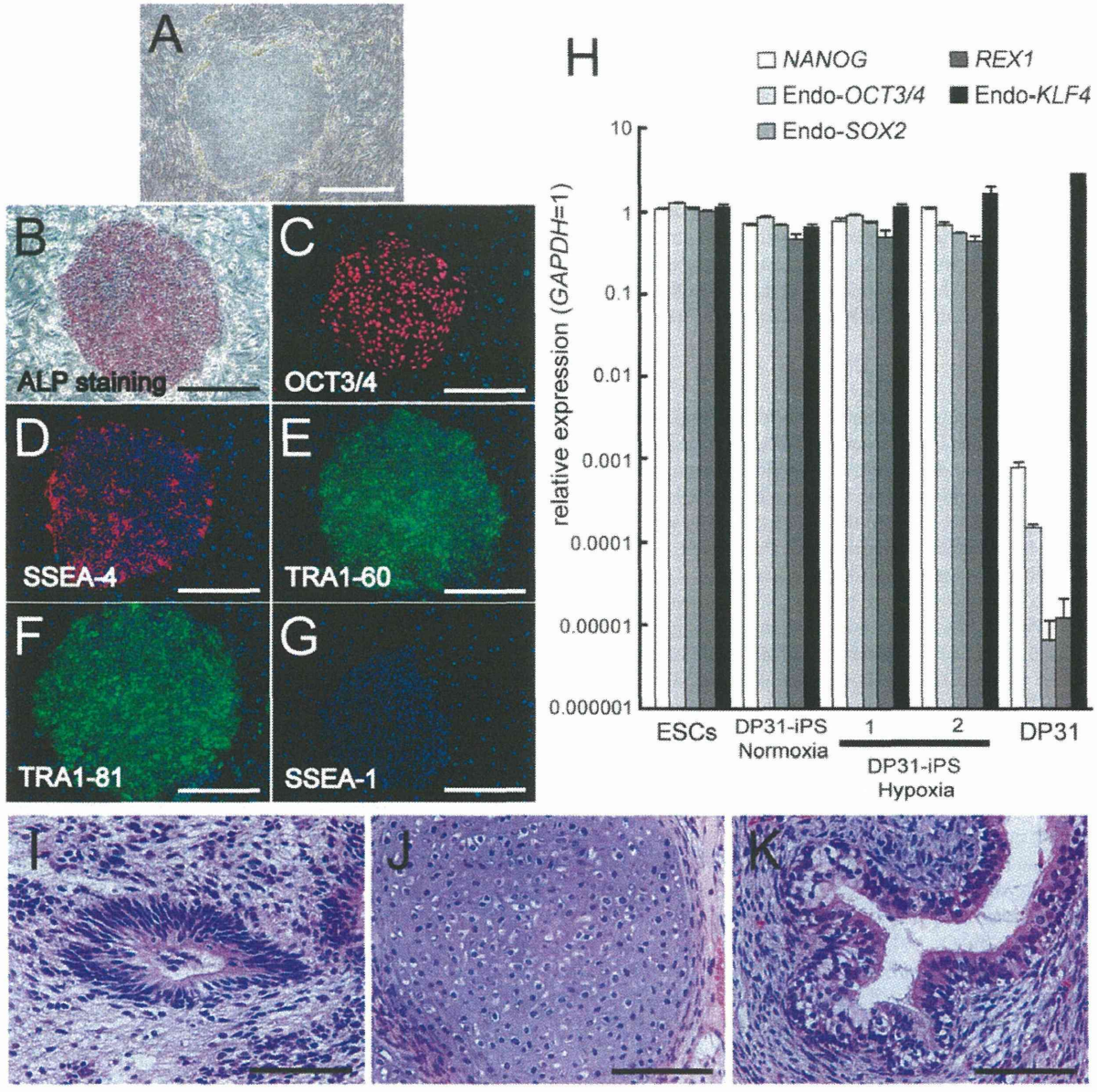

Figure 2. Characterization of iPSCs generated under hypoxic condition. **(A)** Typical morphology of an iPSC colony generated from DP31 under hypoxia (DP31-iPS-1). Scale bar = 200 μm. **(B–G)** iPSCs generated from DP31 under hypoxia (DP31-iPS-1) expressed ALP (B) and pluripotency markers OCT3/4 (C), SSEA-4 (D), TRA1-60 (E), and TRA1-81 (F), but not SSEA-1 (G), as judged by immunostaining. Nuclei were stained with DAPI. Scale bar = 200 μm. **(H)** RT-PCR analysis of ESC-marker genes in iPSCs (DP31-iPS-1 and -2) generated from DP31 under hypoxia, iPSCs generated under normoxia, human ESCs, and DP31. Numbers indicate different iPSC clones generated from DP31. Endogenous *NANOG, OCT3/4, SOX2, REX1,* and *KLF4* were expressed in 2 iPSCs lines generated under hypoxia as well as in human ESCs and iPSCs generated under normoxia, but not in DPCs. Error bars indicate the SD calculated from triplicates. **(I–K)** To confirm the pluripotency of iPSCs generated from DP31 exposed to hypoxia (DP31-iPS-1), we injected the cells into the testes of immunodeficient nude mice to generate teratomas. Twelve wks after injection, we observed tumor formation. Hematoxylin- and eosin-stained teratoma sections show that the tumor contained various types of tissues, such as neural-tube-like structures (I, ectoderm tissue), cartilage (J, mesoderm tissue), and gut-like epithelial tissues (K, endoderm tissue). Scale bar = 200 μm.

of 21 genes increased at least 5-fold (Table 1). Activation of epithelial and inhibition of mesenchymal genes (mesenchymal-epithelial transition, MET) is required for reprogramming mesenchymal cells into iPSCs (Li *et al.*, 2010). *CDH1* (E-cadherin) is an epithelial gene required for reprogramming (Chen *et al.*, 2010; Li *et al.*, 2010). Therefore, we further confirmed the expression of E-cadherin using RT-PCR, suggesting that MET was stimulated in DPCs by hypoxia (Fig. 3A). In contrast, the expression of 10 genes decreased. *CXCR3*, which encodes a chemokine receptor, was down-regulated (Fig. 3B). It should be noted that E-cadherin was significantly down-regulated in hypoxia without introduction of reprogramming factors. We

assume that hypoxia supported the MET in the presence but not the absence of reprogramming factors.

Mir-302 is predominantly expressed in human ESCs or iPSCs, mediates reprogramming of somatic cells, and is up-regulated in hypoxia (Suh *et al.*, 2004; Wilson *et al.*, 2009; Lin *et al.*, 2011; Foja *et al.*, 2013). We determined microRNA levels using microarray analyses of DPCs cultured under conditions of normoxia or hypoxia for 7 days (Appendix Table 3). Mir-302 was not detected in either case; however, Mir-210 was up-regulated over 2-fold in hypoxia, which is regulated by HIF-1α in a variety of tumor types (Huang *et al.*, 2009), suggesting that hypoxia induced changes in the expression of certain microRNAs without affecting that of the ESCs/iPSCs-specific Mir-302.

DISCUSSION

In the present study, we examined the effects of hypoxia on the generation of human iPSCs from DPCs and found that exposure to hypoxia (3% O_2) during the early period of reprogramming (days 1 to day 6) enhanced the induction of ESC-like colonies. Interestingly, when we treated the transfected cells with 3% O_2 during the later stage of reprogramming (from day 6 to day 21), these conditions strongly inhibited the generation of iPSCs. In contrast, a previous study of human DFs exposed to milder hypoxia (5% O_2) in a later period of reprogramming (days 7 to 21 or later) enhanced the generation of iPSCs (Yoshida *et al.*, 2009). Our previous reports showed that iPSC colonies derived from most DPCs lines start to appear by 14 days after retroviral transduction, but human DFs do not start to form any iPSC colonies until 21 days (Tamaoki *et al.*, 2010). Therefore, we conclude from our present findings that exposure to hypoxia from days 1 through 6 after retroviral transduction conforms to the reprogramming schedule of DPCs.

We do not know why prolonged culture under hypoxic conditions strongly inhibited colony formation and growth of maturing iPSCs at late stages of reprogramming. The proliferation of DPCs was optimum in 3% O_2, and DPCs are known to resist hypoxia in 1% O_2 (Iida *et al.*, 2010). Moreover, 3% O_2 did not affect the proliferation or morphology of established iPSCs. Therefore, we assume that hypoxia (3% O_2) may not be toxic for either DPCs or iPSCs; however, it may instead affect an unstable stage involved in their maturation. Further, although we found that the ROS levels were up-regulated in DPCs in 3% O_2, we could not rescue iPSCs from the inhibitory effects of hypoxia using anti-oxidants (Appendix Figs. 2A-2B). We predict that other factors, such as metabolic changes, may be involved.

E-cadherin is a transmembrane constituent of intercellular adherens junctions that are responsible for maintaining epithelial cohesion (Cavallaro and Christofori, 2004) and has been linked to the control of ESC pluripotency (Chou *et al.*, 2008; Soncin *et al.*, 2009). Li *et al.* (2010) reported that exogenous reprogramming factors activate an epithelial program and inhibit expression of key mesenchymal genes to overcome the MET epigenetic barrier of fibroblasts and allow for their successful reprogramming into iPSCs. The gene encoding E-cadherin is activated by *KLF4* expression during reprogramming and is required for generating iPSCs (Chen *et al.*, 2010; Li *et al.*, 2010). In our present study, the expression levels of E-cadherin and *KLF4* in DPCs that were not transduced with reprogramming factors did not increase under

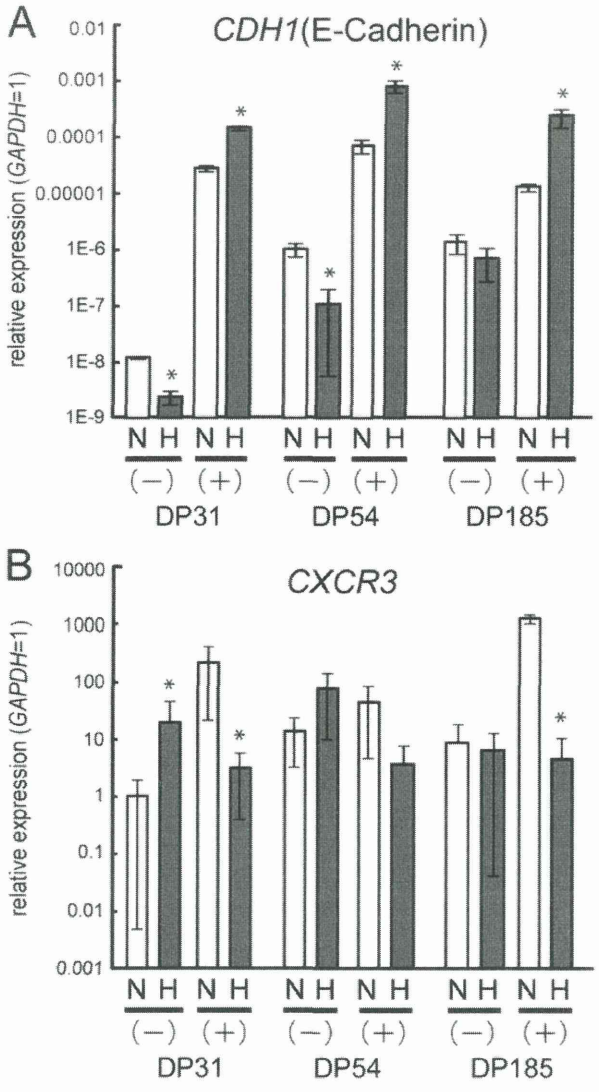

Figure 3. Comparison of the expression levels of *CDH1* (E-cadherin) and *CXCR3* in DPCs exposed to normoxia and hypoxia. DPCs from the three donors were transduced (+) or not (-) as described in "Methods" and then cultured for 6 days under 21% O_2 (N) or 3% O_2 (H). Expression levels of *CDH1* **(A)** and *CXCR3* **(B)** mRNA were assessed by RT-PCR at day 6 post-infection. The mRNA values were divided by those of *GAPDH* and used to calculate expression coefficients. Error bars indicate the SD obtained from triplicate measurements; $*p < .05$ compared with 21% O_2.

hypoxia (*KLF4* data not shown). However, in the presence of reprogramming factors, the expression level of E-cadherin significantly increased. This result in the presence and absence of reprogramming factors is quite interesting because it may indicate that hypoxia affected the early stage of the reprogramming sequence rather than competency of DPCs by changing the expression of E-cadherin and inducing MET.

Microarray analysis revealed that some genes were up-regulated over 10-fold in hypoxia (Table 1). CBLC belongs to the Cbl family of ubiquitin ligases that plays a critical role in protein tyrosine kinase signaling and is exclusively expressed in

epithelial cells, and it may play a role in the MET (Griffiths *et al.*, 2003; Ryan *et al.*, 2012). EGLN3 belongs to the EGLN family of oxygen-sensitive prolyl hydroxylase that controls the degradation of HIF-1α (Epstein *et al.*, 2001). Remarkably, our analysis of microarrays suggested that hypoxia induced changes in the expression levels of several genes encoding chemokines and their receptors (Table 1 and Appendix Figs. 3, 4). Chemokine signaling pathways influence reprogramming target cells toward iPSCs, and the expression of *CCL2*, which encodes a chemokine, dramatically promoted the reprogramming of fibroblasts toward iPSCs (Nagamatsu *et al.*, 2012). Although analysis of our data showed a decrease in *CCL2* expression in hypoxia (Appendix Fig. 4B), the levels of transcription of multiple chemokines and their receptors were altered. Such modulation of chemokine genes may be related to a response of DPCs to inflammation of the teeth, causing signal propagation to the cytokine network (Horst *et al.*, 2011). Interestingly, *CCR4, CCL23*, and *CXCL6*, whose expression levels were altered (Table 1 and Appendix Figs. 3, 4), are expressed at levels 100-fold higher in the odontoblast layer affected by caries (Horst *et al.*, 2011). *IL8*, down-regulated in hypoxia (Table 1), is also an important inflammatory signal mediator. The comparison between up-regulated and down-regulated chemokines and their receptors and examination of downstream signals may reveal the mechanism that underlies the enhanced reprogramming of DPCs observed here.

In the present study, transient hypoxia improved the efficiency of generating iPSCs from DPCs. These conditions differed from those described in a previous report on human DFs. This indicates that complex mechanisms are involved in the effects of hypoxia on the reprogramming process, and that studies conducted *in vitro* must be carefully optimized for each cell type.

ACKNOWLEDGMENTS

We thank the members of the Department of Tissue and Organ Development and the Department of Oral and Maxillofacial Sciences of Gifu University Graduate School of Medicine, and the Center for iPS Cell Research and Application of Kyoto University for their technical help and fruitful discussions. This work was supported by grants from the Ministry of Education, Science, and Culture of Japan, and the JST Yamanaka iPS Cell Project. The authors declare no potential conflicts of interest with respect to the authorship and/or publication of this article.

REFERENCES

Cavallaro U, Christofori G (2004). Cell adhesion and signalling by cadherins and Ig-CAMs in cancer. *Nat Rev Cancer* 4:118-132.

Chen T, Yuan D, Wei B, Jiang J, Kang J, Ling K, *et al.* (2010). E-cadherin-mediated cell-cell contact is critical for induced pluripotent stem cell generation. *Stem Cells* 28:1315-1325.

Chou YF, Chen HH, Eijpe M, Yabuuchi A, Chenoweth JG, Tesar P, *et al.* (2008). The growth factor environment defines distinct pluripotent ground states in novel blastocyst-derived stem cells. *Cell* 135:449-461.

D'Ippolito G, Diabira S, Howard GA, Roos BA, Schiller PC (2006). Low oxygen tension inhibits osteogenic differentiation and enhances stemness of human MIAMI cells. *Bone* 39:513-522.

Epstein AC, Gleadle JM, McNeill LA, Hewitson KS, O'Rourke J, Mole DR, *et al.* (2001). *C. elegans* EGL-9 and mammalian homologs define a family of dioxygenases that regulate HIF by prolyl hydroxylation. *Cell* 107:43-54.

Foja S, Jung M, Harwardt B, Riemann D, Pelz-Ackermann O, Schroeder IS (2013). Hypoxia supports reprogramming of mesenchymal stromal cells via induction of embryonic stem cell-specific microRNA-302 cluster and pluripotency-associated genes. *Cell Reprogram* 15:68-79.

Griffiths EK, Sanchez O, Mill P, Krawczyk C, Hojilla CV, Rubin E, *et al.* (2003). Cbl-3-deficient mice exhibit normal epithelial development. *Mol Cell Biol* 23:7708-7718.

Gronthos S, Mankani M, Brahim J, Robey PG, Shi S (2000). Postnatal human dental pulp stem cells (DPSCs) in vitro and in vivo. *Proc Natl Acad Sci USA* 97:13625-13630.

Gronthos S, Brahim J, Li W, Fisher LW, Cherman N, Boyde A, *et al.* (2002). Stem cell properties of human dental pulp stem cells. *J Dent Res* 81:531-535.

Horst OV, Horst JA, Samudrala R, Dale BA (2011). Caries induced cytokine network in the odontoblast layer of human teeth. *BMC Immunol* 12:9.

Huang X, Ding L, Bennewith KL, Tong RT, Welford SM, Ang KK, *et al.* (2009). Hypoxia-inducible mir-210 regulates normoxic gene expression involved in tumor initiation. *Mol Cell* 35:856-867.

Iida K, Takeda-Kawaguchi T, Tezuka Y, Kunisada T, Shibata T, Tezuka K (2010). Hypoxia enhances colony formation and proliferation but inhibits differentiation of human dental pulp cells. *Arch Oral Biol* 55:648-654.

Li R, Liang J, Ni S, Zhou T, Qing X, Li H, *et al.* (2010). A mesenchymal-to-epithelial transition initiates and is required for the nuclear reprogramming of mouse fibroblasts. *Cell Stem Cell* 7:51-63.

Lin SL, Chang DC, Lin CH, Ying SY, Leu D, Wu DT (2011). Regulation of somatic cell reprogramming through inducible mir-302 expression. *Nucleic Acids Res* 39:1054-1065.

Nagamatsu G, Saito S, Kosaka T, Takubo K, Kinoshita T, Oya M, *et al.* (2012). Optimal ratio of transcription factors for somatic cell reprogramming. *J Biol Chem* 287:36273-36282.

Okita K, Matsumura Y, Sato Y, Okada A, Morizane A, Okamoto S, *et al.* (2011). A more efficient method to generate integration-free human iPS cells. *Nat Methods* 8:409-412.

Packer L, Fuehr K (1977). Low oxygen concentration extends the lifespan of cultured human diploid cells. *Nature* 267:423-425.

Ryan PE, Kales SC, Yadavalli R, Nau MM, Zhang H, Lipkowitz S (2012). Cbl-c ubiquitin ligase activity is increased via the interaction of its RING finger domain with a LIM domain of the paxillin homolog, Hic 5. *PloS One* 7:e49428.

Soncin F, Mohamet L, Eckardt D, Ritson S, Eastham AM, Bobola N, *et al.* (2009). Abrogation of E-cadherin-mediated cell-cell contact in mouse embryonic stem cells results in reversible LIF-independent self-renewal. *Stem Cells* 27:2069-2080.

Suh MR, Lee Y, Kim JY, Kim SK, Moon SH, Lee JY, *et al.* (2004). Human embryonic stem cells express a unique set of microRNAs. *Dev Biol* 270:488-498.

Takahashi K, Tanabe K, Ohnuki M, Narita M, Ichisaka T, Tomoda K, *et al.* (2007). Induction of pluripotent stem cells from adult human fibroblasts by defined factors. *Cell* 131:861-872.

Takeda T, Tezuka Y, Horiuchi M, Hosono K, Iida K, Hatakeyama D, *et al.* (2008). Characterization of dental pulp stem cells of human tooth germs. *J Dent Res* 87:676-681.

Tamaoki N, Takahashi K, Tanaka T, Ichisaka T, Aoki H, Takeda-Kawaguchi T, *et al.* (2010). Dental pulp cells for induced pluripotent stem cell banking. *J Dent Res* 89:773-778.

Watanabe K, Ueno M, Kamiya D, Nishiyama A, Matsumura M, Wataya T, *et al.* (2007). A ROCK inhibitor permits survival of dissociated human embryonic stem cells. *Nat Biotechnol* 25:681-686.

Wilson KD, Venkatasubrahmanyam S, Jia F, Sun N, Butte AJ, Wu JC (2009). MicroRNA profiling of human-induced pluripotent stem cells. *Stem Cells Dev* 18:749-758.

Yoshida Y, Takahashi K, Okita K, Ichisaka T, Yamanaka S (2009). Hypoxia enhances the generation of induced pluripotent stem cells. *Cell Stem Cell* 5:237-241.

Yu CY, Boyd NM, Cringle SJ, Alder VA, Yu DY (2002). Oxygen distribution and consumption in rat lower incisor pulp. *Arch Oral Biol* 47:529-536.

OPEN ACCESS Freely available online

PLoS one

Alterations of Gene Expression and Glutamate Clearance in Astrocytes Derived from an MeCP2-Null Mouse Model of Rett Syndrome

Yasunori Okabe[1,2], Tomoyuki Takahashi[1,3]*, Chiaki Mitsumasu[1,3], Ken-ichiro Kosai[1,3,4], Eiichiro Tanaka[1,2], Toyojiro Matsuishi[1,3]

1 Division of Gene Therapy and Regenerative Medicine, Cognitive and Molecular Research Institute of Brain Diseases, Kurume University, Kurume, Japan, **2** Department of Physiology, Kurume University of Medicine, Kurume, Japan, **3** Department of Pediatrics, Kurume University of Medicine, Kurume, Japan, **4** Department of Gene Therapy and Regenerative Medicine, Advanced Therapeutics Course, Kagoshima University Graduate School of Medical and Dental Sciences, Kagoshima, Japan

Abstract

Rett syndrome (RTT) is a neurodevelopmetal disorder associated with mutations in the methyl-CpG–binding protein 2 (MeCP2) gene. MeCP2-deficient mice recapitulate the neurological degeneration observed in RTT patients. Recent studies indicated a role of not only neurons but also glial cells in neuronal dysfunction in RTT. We cultured astrocytes from MeCP2-null mouse brain and examined astroglial gene expression, growth rate, cytotoxic effects, and glutamate (Glu) clearance. Semi-quantitative RT-PCR analysis revealed that expression of astroglial marker genes, including GFAP and S100β, was significantly higher in MeCP2-null astrocytes than in control astrocytes. Loss of MeCP2 did not affect astroglial cell morphology, growth, or cytotoxic effects, but did alter Glu clearance in astrocytes. When high extracellular Glu was added to the astrocyte cultures and incubated, a time-dependent decrease of extracellular Glu concentration occurred due to Glu clearance by astrocytes. Although the shapes of the profiles of Glu concentration versus time for each strain of astrocytes were grossly similar, Glu concentration in the medium of MeCP2-null astrocytes were lower than those of control astrocytes at 12 and 18 h. In addition, MeCP2 deficiency impaired downregulation of excitatory amino acid transporter 1 and 2 (EAAT1/2) transcripts, but not induction of glutamine synthetase (GS) transcripts, upon high Glu exposure. In contrast, GS protein was significantly higher in MeCP2-null astrocytes than in control astrocytes. These findings suggest that MeCP2 affects astroglial genes expression in cultured astrocytes, and that abnormal Glu clearance in MeCP2-deficient astrocytes may influence the onset and progression of RTT.

Citation: Okabe Y, Takahashi T, Mitsumasu C, Kosai K-i, Tanaka E, et al. (2012) Alterations of Gene Expression and Glutamate Clearance in Astrocytes Derived from an MeCP2-Null Mouse Model of Rett Syndrome. PLoS ONE 7(4): e35354. doi:10.1371/journal.pone.0035354

Editor: Nicoletta Landsberger, University of Insubria, Italy

Received October 26, 2011; **Accepted** March 14, 2012; **Published** April 20, 2012

Funding: This work was supported in part by a Grant-in-Aid for Scientific Research (C) and a Grant-in-Aid for Young Scientists (B) from the Japan Society for the Promotion of Science. The funders had no role in study design, data collection and analysis, decision to publish, or preparation of the manuscript.

Competing Interests: The authors have declared that no competing interests exist.

* E-mail: takahashi_tomoyuki@kurume-u.ac.jp

Introduction

Rett syndrome (RTT) is a neurodevelopmetal disorder that affects one in 15,000 female births, and represents a leading cause of mental retardation and autistic behavior in girls [1,2]. Mutations in the methyl-CpG–binding protein 2 (MeCP2) gene, located in Xq28, have been identified as the cause for the majority of clinical RTT cases [3]. Knockout mouse models with disrupted MeCP2 function mimic many key clinical features of RTT, including normal early postnatal life followed by developmental regression that results in motor impairment, irregular breathing, and early mortality [4,5,6]. MeCP2 dysfunction may thus disrupt the normal developmental or/and physiological program of gene expression, but it remains unclear how this might result in a predominantly neurological phenotype.

In several RTT mouse models, a conditional knockout that is specific to neural stem/progenitor cells or postmitotic neurons results in a phenotype that is similar to the ubiquitous knockout, suggesting that MeCP2 dysfunction in the brain and specifically in neurons underlies RTT [1,6,7]. Recent studies have demonstrated that mice born with RTT can be rescued by reactivation of neuronal MeCP2 expression, suggesting that the neuronal damage can be reversed [1,6]. In addition, several studies using in vitro cell culture systems also indicate that MeCP2 may play a role in processes of neuronal maturation including dendritic growth, synaptogenesis, and electrophysiological responses [1,7]. These data support the idea that MeCP2 deficiency in neurons is sufficient to cause an RTT-like phenotype. However, emerging evidence now indicates that MeCP2 deficiency in glia may also have a profound impact on brain function [8,9,10,11,12,13]. Brain magnetic resonance (MR) studies in MeCP2-deficient mice demonstrated that metabolism in both neurons and glia is affected [8]. Furthermore, in vitro co-culture studies have shown that MeCP2-deficient astroglia non-cell-autonomously affect neuronal dendritic growth [9,10]. In addition, MeCP2-deficient microglia cause dendritic and synaptic damage mediated by elevated glutamate (Glu) release [11]. Very recent studies have indicated that re-expression of MeCP2 in astrocytes of MeCP2-deficient mice significantly improves locomotion, anxiety levels, breathing patterns, and average lifespan, suggesting that astrocyte dysfunc-

tion may be involved in the neuropathology and characteristic phenotypic regression of RTT [13].

Astrocytes regulate the extracellular ion content of the central nervous systems (CNS); they also regulate neuron function, via production of cytokines, and synaptic function, by secreting neurotransmitters at synapses [14,15]. Moreover, a major function of astrocytes is efficient removal of Glu from the extracellular space, a process that is instrumental in maintaining normal interstitial levels of this neurotransmitter [16]. Glu is a major excitatory amino acid; excess Glu causes the degeneration of neurons and/or seizures observed in various CNS diseases [14,17]. RTT is also associated with abnormalities in Glu metabolism, but these findings are controversial due to the limitations of the experimental strategies used. Two studies have demonstrated that Glu is elevated in the cerebrospinal fluid (CSF) of RTT patients [18,19]. MR spectroscopy in RTT patients also revealed elevations of the Glu and Gln peak [20,21]. On the other hand, an animal MR study reported that the levels of Glu and Gln were decreased in a mouse model of RTT [8]. A more recent study indicated that MeCP2-null mice have reduced levels of Glu, but elevated levels of Gln, relative to their wild-type littermates [22]. Another study reported increased Gln levels and Gln/Glu ratios in Mecp2 mutant mice, but no decreases in Glu levels [23]. Although these in vivo studies have explored the hypothesis that the Glu metabolic systems might be altered in RTT, no solid conclusions have yet been reached [24,25].

In this study, we investigated the contribution of MeCP2 to the physiological function of astrocytes. Our studies demonstrate that MeCP2 is not essential for the growth and survival of astrocytes, but is involved in astrocytic Glu metabolism via the regulation of astroglial gene expression.

Results

Characterization of MeCP2-null astrocytes

It was recently reported that MeCP2 is normally present not only in neurons but also in glia, including astrocytes, oligodenrocytes, and microglia [9,10,11]. To determine the roles of MeCP2 in astrocytes, we cultured cerebral cortex astrocytes from both wild-type ($MeCP2^{+/y}$) and MeCP2-null ($MeCP2^{-/y}$) mouse brains (Fig. 1). MeCP2-null astrocytes exhibited a large, flattened, polygonal shape identical to that of the wild-type astrocytes, suggesting that normal patterns of cellular recognition and contact were present. Semi-quantitative RT-PCR using primer sets that specifically amplify two splice variants, Mecp2 e1 and e2, showed that control astrocytes expressed Mecp2 e1 and e2, whereas neither Mecp2 variant was detectable in MeCP2-null astrocytes (Fig. 1A). We further confirmed expression of MeCP2 by immunocytochemical staining of astrocytes. In control samples, almost all GFAP-positive cells exhibited clear nuclear MeCP2 immunoreactivity in astrocytes, but no immunoreactivity was observed in MeCP2-null astrocytes (Fig. 1B).

MeCP2 has been reported to be involved in regulation of astroglial gene expression [26,27]. Consistent with this, GFAP levels were significantly higher in MeCP2-null astrocytes (Fig. 1A). Similarly, the expression of S100β, another astrocyte maturation marker, was significantly upregulated by MeCP2 deficiency (fold change of control = 1.0, GFAP: 2.195±0.504, n = 4 each, $p<0.05$; S100β: 2.779±0.329, n = 4 each, $p<0.01$). These results show that MeCP2 deficiency upregulates astroglial gene expression in astrocytes.

To compare the growth of the wild-type and MeCP2-null astrocytes, we counted total cell number at each passage (Fig. 2A). As passage number increased, the cell growth rate decreased dramatically for both types of astrocytes, ultimately culminating in senescence. There was no significant difference in growth rate between the control and MeCP2-null astrocyte cultures. We then measured astrocyte proliferation via BrdU incorporation assay (Fig. 2B and Fig. S1). After 2 h of BrdU treatment, the proportions of BrdU-incorporating cells were similar in the control and MeCP2-null astrocytes (6.635±1.655% in control versus 6.774±2.272% in MeCP2-null astrocytes, n = 4 each, p = 0.962). These results suggest that the absence of MeCP2 did not affect the proliferation of astrocytes in our culture condition.

We also tested the cytotoxic effects of hydrogen peroxide (H_2O_2), ammonium chloride (NH_4Cl), and glutamate (Glu), on astrocytes in our culture (Fig. 2C–E). In cultures derived from both wild-type and MeCP2-null strains, cell viability decreased with increasing concentrations of H_2O_2 and NH_4Cl. In contrast, in our culture conditions, we observed virtually 100% viability of both the control and MeCP2-null astrocytes after 24 h incubation with 10 mM Glu. Glu-induced gliotoxic effects have been previously reported by Chen et al. (2000), and are probably due to distinct differences in culture conditions, specifically the presence of glucose [28]. These results showed that H_2O_2 and NH_4Cl had a similar effect in both strains of astrocytes. There was no significant difference in viability between the control and MeCP2-null astrocyte cultures, indicating that MeCP2 deficiency did not affect astrocyte viability upon treatment with H_2O_2 and NH_4Cl.

Effects of glutamate on glutamate transporters and glutamine synthetase transcripts in MeCP2-null astrocytes

High extracellular Glu interferes with the expression of the astrocyte transporter subtypes, excitatory amino acid transporter 1(EAAT1)/glutamate/aspartate transporter (GLAST) and EAAT2/glutamate transporter-1 (GLT-1) [16,29]. To explore the effects of Glu on the expression of Glu transporter genes in cultured astrocytes from wild-type and MeCP2-null mouse brains, we asked whether treatment with 1.0 mM Glu altered expression of EAAT1 and EAAT2 mRNA, using a semi-quantitative RT-PCR assay (Fig. 3). EAAT1 and EAAT2 mRNA were expressed in both wild-type and MeCP2-null astrocytes, and were slightly higher in controls than in MeCP2-null astrocytes. Both EAAT1 and EAAT2 mRNA levels were altered in the control astrocytes after treatment with 1.0 mM Glu. EAAT1 mRNA levels decreased significantly in the wild-type astrocytes, both 12 h and 24 h after treatment with Glu (Fig. 3A). In contrast, EAAT1 decreased significantly in the MeCP2-null astrocytes, at 12 h but not 24 h after treatment. As with EAAT1, EAAT2 mRNA levels also decreased significantly in the control astrocytes, both 12 h and 24 h after treatment (Fig. 3B). However, EAAT2 decreased significantly in MeCP2-null astrocytes, 24 h but not 12 h after treatment. In addition, the effects of Glu on EAAT1 and EAAT2 relative fold expression at 12 h were altered in the MeCP2-null astrocytes (Fig. 3D: EAAT1; 0.618±0.033 in control versus 0.758±0.049 in MeCP2-null astrocytes, n = 10 each, $p<0.05$; Fig. 3E: EAAT2; 0.794±0.055 in control versus 0.964±0.048 in MeCP2-null astrocytes, n = 8 each, $p<0.05$). These results suggest that the loss of MeCP2 leads to transcriptional dysregulation of these genes, either directly or indirectly.

One important enzyme that plays a role in the Glu metabolic pathway is glutamine synthetase (GS) [17,29]. GS is mainly located in astrocytes; cultured astrocytes response to Glu with increased GS expression [17,29]. Consistent with this, 1.0 mM Glu treatment stimulated GS mRNA expression in both the wild-type and MeCP2-null astrocytes about 1.2-fold after 12 h but not 24 h (Fig. 3C). In addition, MeCP2 deficiency did not modify the

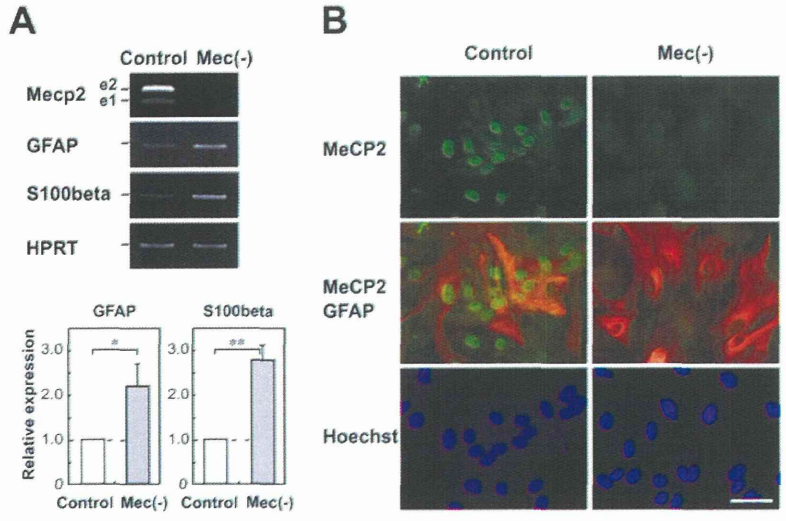

Figure 1. Characterization of assay cultures. A. Expression of astroglial genes in primary cultured cortical astrocytes. Semi-quantitative RT-PCR analysis of Mecp2 and astroglial genes was performed in wild-type (white column) and MeCP2-null (gray column) astrocytes. Mecp2 e1 and e2 were detectable in the wild-type astrocytes. The lower graphs show that the GFAP/HPRT or S100β/HPRT expression ratio in each genotype was normalized against the level in control astrocytes. Bars represent the means ± standard errors (SE) of samples from three independent experiments (*$p<0.05$). The expression of astroglial markers was significantly upregulated by MeCP2 deficiency. **B.** Expression of MeCP2 in the primary cultured cortical astrocytes. The astrocytes were immunostained with MeCP2 (green) and GFAP (red) as glial-specific astrocytic markers. Scale bars indicate 50 μm.
doi:10.1371/journal.pone.0035354.g001

effects of Glu on GS mRNA relative fold expression in cultured astrocytes (Fig. 3F, 1.245±0.054 in control versus 1.265±0.093 in MeCP2-null astrocytes, n = 6 each, p = 0.859). These results suggested that MeCP2 did not modify the expression of GS in the cultured astrocytes. Overall, the expression levels of GS mRNA did not differ between both strains of astrocytes following treatment with Glu.

Comparison of glutamate clearance between wild-type and MeCP2-null astrocytes

Because MeCP2 contributed to the transcriptional regulation of Glu metabolism-related genes in our culture systems, we next compared the Glu clearance capability of the wild-type and MeCP2-null astrocytes (Fig. 4A). The cell culture supernatants in both astrocyte cultures were collected at 3–24 h post incubation in culture media containing 1.0 mM Glu. After incubation in culture medium containing Glu, we identified a time-dependent reduction in Glu over 24 h of incubation in both strains of astrocytes. Although the shapes of the profiles of Glu concentration versus time for each strain of astrocytes were grossly similar, Glu concentration in the medium of MeCP2-null astrocytes were lower than those of control astrocytes at 12 and 18 h (12 h: control, 0.513±0.052 mM versus MeCP2-null, 0.395±0.022 mM, $p<0.05$; 18 h: control, 0.368±0.029 mM versus MeCP2-null, 0.125±0.007 mM, $p<0.01$, n = 6 each, Fig. 4A). The differences in Glu clearance were not due to changes in cell death of control astrocytes upon application of Glu (Fig. 2E). This indicates that Glu clearance by MeCP2-null astrocytes was more efficient than by control astrocytes.

The Glu transporters EAAT1 and EAAT2 are located primarily on astrocytes and are critical in maintaining extracellular Glu at safe levels [16]. Threo-beta-benzyloxyaspartate (TBOA) is a broad-spectrum glutamate transporter antagonist, affecting EAAT1 and EAAT2 [30]. UCPH-101 (2-amino-4-(4-methoxyphenyl)-7-(naphthalen-1-yl)-5-oxo-5,6,7,8-tetrahydro-4H-chromene-3-carbonitrile) and dihydrokainate (DHKA) are selective inhibitors for EAAT1 and EAAT2, respectively [30,31]. To investigate the functional Glu transporters in our astrocyte cultures, we analyzed three Glu transporter blockers (TBOA, UCPH-101, or DHKA) for their ability to alter the effects of Glu clearance (Fig. 4B–D). Glu clearance by the wild-type astrocytes was partially blocked by addition of TBOA and UCPH-101, but not DHKA. This suggests that EAAT1, but not EAAT2, plays a major role in Glu clearance under our astroglial culture conditions.

Effects of glutamate on glutamine synthetase and EAAT1 protein in MeCP2-null astrocytes

The initial set of experiments aimed to determine whether Glu modulate the translation of GS and EAAT1 protein (Fig. 5 and Fig. S2). GS protein was expressed in both wild-type and MeCP2-null astrocytes, and was significantly more abundant in MeCP2-null astrocytes (Fig. 5B: fold change of control = 1.0, 2.631±0.368, $p<0.01$). After 12 h exposure to 0.01–1.0 mM Glu, wild-type astrocytes exhibited a dose-dependent increase in GS protein levels (about 6-fold in 1.0 mM Glu treatment). Similar to its effect on the wild-type astrocytes, in the MeCP2-null astrocytes Glu exposure dose-dependently increased GS protein levels relative to untreated astrocytes (Fig. S2). We then examined the effect of 1.0 mM Glu on levels of GS protein, over a time course (Fig. 5A). GS expression was highest after 12 h exposure to 1.0 mM Glu, decreasing slightly by 24 h in both wild-type and MeCP2-null astrocytes. Densitometric analysis of the bands in three independent experiments demonstrated that GS protein in MeCP2-null astrocyte cultures was higher than in wild-type astrocytes, 12 h but not 24 h after treatment (Fig. 5B: fold change of control = 1.0, at 12 h: 1.421±0.139, $p<0.05$; at 24 h: 1.131±0.130, p = 0.354, n = 4 each). These results indicated that MeCP2 deficiency caused higher expression of GS protein in cultured astrocytes.

We also asked whether treatment with 1.0 mM Glu altered expression of EAAT1 protein. EAAT1 protein was expressed in

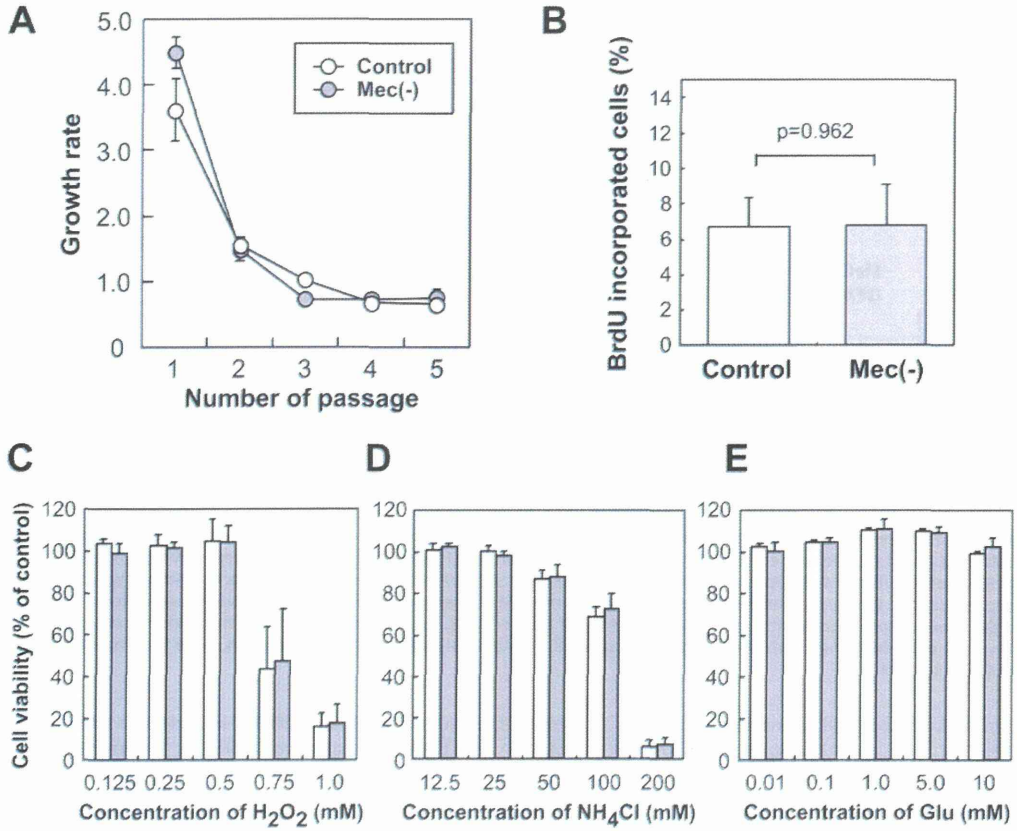

Figure 2. Cell growth and viability. A. Comparison of cell growth in wild-type and MeCP2-deficient astrocytes. As passage number increased, cell growth rate decreased dramatically in both strains of astrocytes. There was no significant difference in growth rate between the control and MeCP2-null astrocyte cultures. **B.** Quantification of BrdU-incorporating cells in control and MeCP2-null astrocytes. Astrocytes were cultured for 24 h and incubated with BrdU for 2 h. The graph shows the percentage of BrdU-incorporating cells in the control (white column) and MeCP2-deficient (gray column) astrocytes 2 h after BrdU exposure. The number of BrdU-incorporating cells is expressed as a percentage of the total number of Hoechst-stained cells (Fig. S1). Bars represent the means ± SE of the samples from four independent experiments. The ratio of BrdU-incorporating cells is similar in astrocytes taken from both control and MeCP2-null strains. **C–E.** Comparison of effects of various neurotoxins (**C,** H_2O_2; **D,** NH_4Cl; **E,** Glutamate) on control and MeCP2-null astrocytes. The graph shows the percentage of viability in the control (white column) and MeCP2-deficient (gray column) astrocytes after neurotoxin treatment at the indicated concentrations. Bars represent the means ± SE of samples from three independent experiments. The glial cultures showed no difference in viability between the control and MeCP2-null strains.
doi:10.1371/journal.pone.0035354.g002

both wild-type and MeCP2-null astrocytes, at levels that were similar in controls and MeCP2-null astrocytes. EAAT1 protein levels were altered in the wild-type astrocytes after treatment with 1.0 mM Glu. EAAT1 protein levels decreased significantly in the wild-type astrocytes, 24 h but not 12 h after treatment (Fig. 5C). In contrast, EAAT1 did not decrease in the MeCP2-null astrocytes, either 12 h or 24 h after treatment. In addition, the relative expression levels of EAAT1 24 h after treatment were lower in the wild-type than in the MeCP2-null culture, although the difference was not statistically significant (Fig. 5D: 12 h; 1.102±0.169 in control versus 1.096±0.142 in MeCP2-null astrocytes, n = 6 each, p = 0.979, 24 h; 0.456±0.123 in control versus 0.901±0.172 in MeCP2-null astrocytes, n = 5 each, p = 0.068). These results suggest that MeCP2 deficiency affects the expression of GS and EAAT1 protein, and that accelerated Glu clearance may result from dysregulation of GS and EAAT1 protein in MeCP2-null astrocytes.

Discussion

Recent studies suggest that glia, as well as neurons, cause neuronal dysfunction in RTT via non-cell-autonomous effects. Here, we have demonstrated that MeCP2 regulates the expression of astroglial marker transcripts, including GFAP and S100β in cultured astrocytes. In addition, MeCP2 is not essential for the cell morphology, growth, or viability; rather, it is involved in Glu clearance through the regulation of Glu transporters and GS in astrocytes. Altered astroglial gene expression and abnormal Glu clearance by MeCP2-null astrocytes may underlie the pathogenesis of RTT.

In this study, MeCP2-null astrocytes exhibited significantly higher transcripts corresponding to astroglial markers, including GFAP and S100β. Consistent with this, transcription of several astrocytic genes, including GFAP, is upregulated in RTT patients [26,32]. Indeed, MeCP2 binds to a highly methylated region in the GFAP and S100β in neuroepithlial cells [27,33]; ectopic